

Semi-Annual Report  
January, 1966

FACILITY FORM 602

N66-20876	
(ACCESSION NUMBER)	(THRU)
42	1
(PAGES)	(CODE)
CR 71147	17
(NASA CR OR TMX OR AD NUMBER)	(CATEGORY)

ADHESION BETWEEN ATOMICALLY PURE METALLIC SURFACES.

PART IV: ATHE

Prepared for

NASA CR 71147

National Aeronautics and Space Administration

Office of Grants and Research Contracts; Code CS

Washington, D.C.

Submitted by:

Douglas V. Keller, Jr., Director

GPO PRICE \$

CFSTI PRICE(S) \$

Hard copy (HC)

Microfiche (MF)

#653 July 65

This report was produced under a sponsored contract. The conclusions and recommendations expressed are those of the Author and are not necessarily endorsed by the Sponsor. Reproduction of this report, or any portion thereof, must bear reference to the original source and Sponsor.

SYRACUSE UNIVERSITY RESEARCH INSTITUTE

Department of Chemical Engineering and Metallurgy

Approved by:

Sponsored by:

Douglas V. Keller, Jr.  
Project Director

N.A.S.A. - NsG-483  
Supplement 1

S.U.R.I. Report No. Met. 1100-661SA

THE EFFECT OF CONTAMINATION ON THE ADHESION  
OF METALLIC COUPLES IN ULTRA-HIGH VACUUM

by

K. I. Johnson and D. V. Keller, Jr.

Department of Chemical Engineering and Metallurgy

Syracuse University

Syracuse, New York

## ABSTRACT

The presented work is concerned with determining the factors controlling the adhesion of metal couples.

Most previous studies have been done in the presence of contaminants and, under these conditions, an energy barrier for adhesion has always been observed. This barrier has been ascribed to various factors: the need to disperse the contaminants so that metal-metal contact, and, consequently adhesion, can occur; the energy required to realign the surface metal atoms to form an interfacial bond; and, for lightly loaded conditions, the necessity to overcome the elastic relief stresses which may break any bond formed during the unloading of the couple. A further condition for adhesion which has been postulated, is that the metal couples must be mutually soluble.

The present adhesion experiments show that contaminant dispersal is the major barrier to adhesion. Thus, spontaneous adhesion occurred under vacuum conditions for the three systems studied when the surfaces were sufficiently clean, whereas subsequent contamination resulted in non-adhesion. Substantial amounts of contamination could, however, be tolerated. The contaminants may be divided into two classes, stable surface films and mobile gaseous or liquid films. While both are barriers to adhesion, the latter may be removed by application of a vacuum, whereas the former requires a more rigorous treatment.

Because adhesion occurred for clean surfaces under vacuum conditions, even where elastic deformation predominated, the postulated energy barrier of adhesion due to the realignment of the surface atoms is considered of minor importance, at least for the softer metals studied here. Further, no evidence for rupture of the bonds by the elastic relief forces on unloading such lightly loaded clean couples has been observed. The latter effect,

however, is thought to become more important whenever stable surface films are present, because of the limited metal-metal contact.

Since the one immiscible system studied here showed as great a tendency to adhesion as the miscible systems, the condition of bulk miscibility is considered no criterion, per se, for adhesion.

## INTRODUCTION

It is generally accepted (1-3) that contamination is a major barrier to the adhesion of solid-phase metal couples. Thus, the ability of metal pairs to bond after bulk deformation (3) has been found to depend greatly on their initial surface treatment. Similarly, the friction between two metal surfaces, which has been shown by Bowden and Tabor (1) to be due in part to the bonding of surface asperities, is significantly reduced by lubricants.

The exact magnitude of the effect of contaminants on the bond strength of metal couples is, however, unknown since most solid phase welding experiments (3-5) have been conducted in air under complex surface conditions where metal crystal structure, bulk deformation and temperature have all been found to have an effect. Due to the interrelation of all these variables, there is still dispute as to whether dispersal of contaminants or an inherent energy barrier, due to realignment of the surface atoms to form an interfacial bond, is responsible for the dependence of adhesion on bulk deformation (3).

In order to eliminate the effects of contamination, a few attempts have been made to study the adhesion of clean metal surfaces under vacuum. For example, Bowden and Rowe (6) have examined the adhesion of metal couples under normal loading after varying degrees of tangential prestressing. The metals were first cleaned by high temperature evaporation under vacuum, and the tests conducted under a vacuum of about  $10^{-8}$  Torr. The degree of adhesion was less than might be expected and this was originally attributed to the breaking of the interfacial bonds by relief of elastic stresses as the applied load was removed. More recently, however, Milner and Rowe (3) have suggested that contamination of these surfaces could not be ruled out.

Additional impetus has recently been given to the study of solid phase bonding because of the need to foresee and control the seizure of space capsule components operating under deep space conditions, i.e. a vacuum of

about  $10^{-13}$  Torr; and, as a consequence, a number of adhesion studies (7-9) at pressures in the range of below  $10^{-9}$  Torr have been attempted.

Keller and Spalvins (9) reported that mutually soluble metal couples, cleaned by argon and electron bombardment, showed evidence of adhesion under touch contact. Insoluble couples, however, did not appear to demonstrate adhesion. Although no measure of loads or estimations of the resultant metal contact areas were made, the former results did indicate that contaminant dispersal is the major barrier to adhesion. Even though the lack of adhesion of the insoluble couples appears to be in agreement with some observations in friction and wear studies (10,11), this observation is at variance with the roll-bonding work done in the presence of contaminants by McEwan and Milner (12).

In order to elucidate the mechanisms involved in solid metal adhesion, therefore, an experiment was designed to measure the forces involved in the bonding of metal surfaces with varying degrees of cleanliness, under a series of ambient pressures which ranged from 40 Torr to about  $5 \times 10^{-10}$  Torr.

## EXPERIMENTAL PROCEDURE

The adhesion cell and pumping system were designed to allow for the measurement of the contact resistance and adhesion between two metal samples as a function of contact force, with varying degrees of surface contamination. The system used consisted of a 40 x 300 mm pyrex adhesion cell (A) attached to a 1" ultra-high vacuum valve (H) and thence to the vacuum system, as shown in Figure 1. The adhesion cell, valve, and first liquid nitrogen trap were baked-out during each experiment at 450°C for at least 10 hours. After bake-out, the degassing of the titanium sorption pump, and the cooling of the first liquid nitrogen trap, the minimum pressure observed in the adhesion cell was  $5 \times 10^{-10}$  Torr, as measured by the NRC Redhead gauge (D) mounted adjacent to the specimens. The titanium sorption pump (E) consisted of a helix of 0.010" titanium wire closely wrapped over 0.015" tungsten wire.

The torsion beam and adhesion samples are shown in Figure 2. Both were supported by three 5 mm stainless steel support rods heliarc welded to a stainless steel conflat plate attached to the cell at (J), Figure 1. The rods also served as supports for the sample electrical leads within the chamber, which were all insulated with recrystallized alumina tubing and left the cell by standard Kovar through-seals at (B), Figure 1. The torsion beam was also constructed of alumina tubing and was supported at its center by a stainless steel connector which served as a bearing for the torsion beam as it rested on a 0.010" tungsten wire under tension between the two 5 mm stainless steel supports.

The iron slug,  $F_1$ , Figure 2, fixed to the end of the torsion beam, was used in conjunction with the external permanent magnet (C) to affix the position of the indenter with respect to the sample plate. The strain gauge (G) mounted on the torsion beam, supported a second iron slug,  $F_2$ , which

interacted with the field of a solenoid (L). Thus, as the current in the solenoid, monitored by the calibrated variable resistance (J) was increased, the torsion beam was moved into sample contact and a normal force placed on the sample plate due to the indenter. The force of shearing the magnetic flux between the iron slug,  $F_1$ , and the magnet (C) before contact, and the force of contact of the indenter (B) with the fixed sample plate (A) were measured by the 0.00095" x 6" nude straight constantan wire strain gauge, whose output was monitored by a Sanborn Transducer-Amplifier, Model 312. Prior to each experiment the balance system was calibrated in air throughout the range of operation, i.e. 0-2.0 grams, and was found to have a sensitivity of about  $\pm 0.010$  grams.

The contact resistance between the indenter and plate was measured with a Precision Kelvin Bridge in conjunction with a Nanovoltmeter used as a null detector. A source was used such that the potential drop across the contact resistance was approximately 0.3 millivolts, which should yield negligible temperature rise at the contact region due to current flow (13). Such an arrangement enabled the resistance to be measured when within the range of zero to one ohm, with an accuracy of 3-4 figures. The resistance circuit was calibrated with a 0.01 ohm NBS standard resistor prior to each run.

The torsion beam arrangement was designed in the above way in order to obtain, as nearly as possible, pure normal loading. Thus, shear deformation of the adhesion specimens was reduced to a minimum during test cycles, the only tangential motion being imparted to the specimens by unavoidable normal laboratory vibrations. The effects of these could only be observed under extreme light specimen loading and non-adhesion conditions, when instability of the contact resistance occurred.

The normal operating procedure involved placing the samples in the system and evacuating to a pressure below  $10^{-5}$  Torr, at which time the



bakeout cycle was imposed, as previously mentioned, to attain an ultimate pressure of about  $5 \times 10^{-10}$  Torr. At this time the ultra-high purity argon, obtained from Airco Company, was admitted to the leak system by breaking the capsule break-off tip. The argon was then admitted to the cell to a pressure of about  $10^{-4}$  Torr, and argon ion bombardment of each surface initiated by placing a D.C. potential of about a kilovolt between the filament (E), Figure 2, and the surface to be cleaned. During the cleaning operation, which amounted to a total of at least three hours for each surface, a small nickel shield was moved into place (via magnet) to completely shield the surface not being cleaned from contamination by sputtered material. After bombardment, a substantial sputtered deposit on the cell walls attested to the fact that a considerable amount of surface material was removed from each sample. Upon completion of the argon ion bombardment phase, the system was evacuated and sample annealing initiated. Electron bombardment from the filament (E) was used to heat the sample for argon degassing and sample anneal. During this procedure momentary pressure peaks in the range of  $10^{-7}$  Torr were observed, which fell within a few seconds to below  $10^{-9}$  Torr. The ultimate pressure upon completion of this operation, after degassing the thin sputtered film and firing the titanium sorption pump, was about  $5 \times 10^{-10}$  Torr. Damp or dried air (i.e. air dried with silica gel for 3 days) was subsequently admitted to the system by means of the argon reservoir.

At certain points throughout the whole of this evacuation and surface cleaning process a series of adhesion cycles were performed at room temperatures by slowly bringing indenter (B) into contact with (A), by reducing the variable resistance (J). The values of (J) and the deflection of the transducer amplifier, due to the strain gauge, were noted concurrently at discrete intervals until sample contact was made, when contact resistance measurements were also performed at each new adjustment of (J). The load on the adhesion

couple was then further increased to a predetermined level and then reduced by increments until contact was broken. Contact make and break were immediately indicated by a closed and open circuit in the Kelvin Bridge. In this way the loading and unloading processes were monitored by at least ten concurrent contact resistance, force, and solenoid circuit resistance measurements during each adhesion cycle. The peak loads usually included 0.02, 0.15, 0.30, 0.60, 0.80, 1.0 and 1.5 grams, which allowed for an estimation of the effect of peak contact load on metal-metal adhesion.

In the present study the Ag-Ag, mutually soluble Cu-Ni and mutually insoluble Ag-Ni systems (14) were studied. The materials used were: 99.999% silver, 99.97% nickel and O.F.H.C. copper. In the cases where nickel was used a 0.8 cm<sup>2</sup> fixed plate at (A), Figure 2, was employed, with a silver or copper sphere at (B), formed by fusing 1 mm diameter wire into a sphere of about 3 mm diameter. Fusion was done in air with an oxy-hydrogen flame. The Ag-Ag adhesion couple, however, consisted of two crossed 1 mm wires.

## RESULTS AND DISCUSSION

Typical adhesion cycles for the Ag-Ag system are shown in Figure 3. Two examples are given; a specimen showing no adhesion, Figure 3a, and one showing appreciable adhesion, Figure 3b. In the former case contact make and break occur at approximately the same value of  $(J)$  (i.e. at the same attractive force between solenoid and slug,  $F_2$ ), whereas in the latter, the value of  $(J)$  at break is markedly greater than that at make. The differences of the load on the adhesion couple at the same values of  $(J)$ , between the loading and unloading cycles, is not significant as it is due to an observed drift with time of the strain gauge deflection as measured on the transducer-amplifier. This drift can be approximately corrected for by vertically projecting the contact break point onto the loading curve. If this is done, the load to break the adhesion couple in Figure 3a is 0 grams, whereas that in Figure 3b is  $\sim 0.14$  grams. A reasonable approximation of the load applied to the couple in both cases is the load difference between contact make and maximum load.

Thus, one criterion for adhesion of the specimen couples is the presence of a significant load required to separate the contact after loading. Other criteria may be obtained from examination of the load-contact resistance relationship. Thus, marked instability before break, and non-maintenance of minimum resistance during unloading indicate non-adhesion (cf. Figure 3a and b). Further evidence for adhesion could often be observed during the positioning of the indenter by the external magnet (C), Figure 2, when visible adhering to the plate occurred due to an accidental contact of the specimen samples.

### 1. Estimation of Bond Strengths

As may be readily appreciated, a measure of the bond strengths of

the couples showing adhesion is desirable for an understanding of the adhesion process. Thus, since the load to break the couple is easily measurable, an estimation of the contact area for each adhesion cycle is required. This may be approximated from either contact resistance data or from mechanical considerations.

a) Contact Area Approximation by Contact Resistance

If one circular contact region is assumed between two members of the same metal with clean surfaces, the radius of the contact region, and hence its area, can be estimated from the equation as suggested by Holm (15)

$$R = \rho/2a \quad (1)$$

where  $R$  is the contact resistance,  $\rho$  is the specific resistivity of the metal, and  $a$  is the radius of the circular contact zone. If a dissimilar metal couple is present, the formula may be adapted to,

$$R = \rho_1/4a + \rho_2/4a \quad (2)$$

where  $\rho_1$  and  $\rho_2$  are the specific resistivities of the two metals.

It should be noted that the above formulae apply only to clean surfaces; for, if a contaminant film is present, an additional resistance term due to its thickness and resistivity must also be present (15). Consequently, this approach may be applied, with reasonable accuracy, only to the adhesion cycles conducted in ultra-high vacuum, after argon ion and electron bombardment.

Figure 4 shows a plot of the contact resistances at maximum load vs the load on the couple for the systems studied. Each point represents one cycle under the above conditions. It is evident that there is a marked difference between the three

systems in the ranges of resistances observed. Figure 5 further shows a plot of joint strength (contact area estimated from formula (1)) versus load on the couple, for the Ag-Ag system. Although there is much scatter, the bond strengths seem to approximate well to the bulk strength of silver. There seems to be little strength-load dependence since substantial strengths are observed even for loads of 0.1 grams on the couple. When similar calculations are conducted for the Cu-Ni and Ag-Ni results, however, bond strengths consistently of ten to three times those of the bulk strengths of the weaker copper and silver members, respectively, are obtained, which are considered anomalously high.

b) Contact Area Approximation from Mechanical Considerations

In order to approximate the contact area by mechanical considerations, it must be first determined whether the deformation is predominantly elastic or plastic. If the deformation of the adhesion couples is assumed to be totally elastic, and the surfaces are further assumed perfectly flat, or spherical, the contact area may be estimated by using the equation derived by Hertz (16),

$$a = \left[ \frac{3}{4} W \left( \frac{1-\sigma_1^2}{E_1} + \frac{1-\sigma_2^2}{E_2} \right) \left( \frac{1}{r_1} + \frac{1}{r_2} \right)^{-1} \right]^{1/3} \quad (3)$$

where,       $a$  = radius of contact zone  
                $r$  = radius of curvature of couple members  
                $\sigma$  = Poissons ratio  
                $E$  = Young's modulus of elasticity  
                $W$  = load

Consequently, the average pressure under the indenter,  $P_m$ , varies as:

$$P_m = W/\pi a^2 = W/\pi \left[ \frac{3}{4} W \left( \frac{1-\sigma_1^2}{E_1} + \frac{1-\sigma_2^2}{E_2} \right) \left( \frac{1}{r_1} + \frac{1}{r_2} \right)^{-1} \right]^{2/3} \quad (4)$$

If, however, the deformation is assumed to be mainly plastic, as will occur at heavy loads, the mean pressure under the indenter may be approximated (15) from the hardness of the annealed material; i.e.

$$P_m = H \quad (5)$$

Figure 6 shows a plot of  $P_m$  vs load for these two idealized deformation mechanisms, AB representing the variation of Equation (4) and BC of Equation (5).

If we now consider the deformation of the Ag-Ag couple, Equation (4) reduces to,

$$P_m = W^{1/3}/4.07 \times 10^{-7} \text{ grams/cm}^2 \quad (6)$$

by substituting the appropriate values of  $\sigma$ ,  $E$ , and  $r$ . Similarly, Equation (5) reduces to

$$P_m = 48.3 \times 10^5 \text{ grams/cm}^2 \quad (7)$$

since the V.P.N. of the silver specimen was found to be  $48.3 \text{ kg/mm}^2$  (load, 200 grams). Consequently, by combining expressions (6) and (7), one may estimate that  $W_B$ , for the Ag-Ag system, occurs at a load of 7.6 grams. However, this load does not represent the change from elastic to plastic behavior as there is a transition region, AC, Figure 6, in the  $P_m$  - load relationship, where A is the initiation of plastic deformation (17). This latter occurs at  $0.5a$  below the metal surface at a load of  $W_A$ , when,

$$P_m = 1.1 \gamma \quad (8)$$

$y$  being the yield strength of the material.  $W_A$  may thus be calculated for the Ag-Ag system by equating expressions (6) and (8), and is found to be either  $1.5 \times 10^{-2}$  or  $4.2 \times 10^{-5}$  grams depending on the value ascribed to  $y$  (18).

Thus, it seems that, for the adhesion couple which would most tend towards plastic behavior, because of the lower yield stress and the geometry of the specimens, the initiation of plastic yielding occurs at  $10^{-5}$  -  $10^{-2}$  grams, and that there is still appreciable elastic deformation at 7.6 grams load. Thus, since the present series of adhesion cycles have been performed under loads of 0.03 - 2.0 grams, an approximation of the contact area at maximum load may be made by applying Equation (3).

If this is done for the Ag-Ag adhesion cycles performed under high vacuum after bombardment, a joint strength-indentation load relationship is obtained as shown in Figure 7. As can be seen this is very similar to Figure 5, where the contact areas were estimated from contact resistance data. Very high strengths, however, are observed at low loads for the former case, Figure 7. This is thought to be a spurious effect due to a flattened contact area formed during assembly of the torsion balance, by accidental touching of the specimen wires together. Such an occurrence would lead to an underestimation of the contact area by the elastic approximation.

On applying the elastic area approximation to the results obtained from the mutually soluble and insoluble Cu-Ni and Ag-Ni systems, done under the same conditions as above, plots materially the same as that of Figure 7 are obtained, i.e. joint strengths approximating to the strength of the weakest member

(Cu or Ag). Again, no joint strength-load dependence is apparent. These strengths are considered to be more reasonable than those obtained for the dissimilar couples from contact areas derived via their contact resistances. It must be assumed, therefore, that the measured resistances of the Cu-Ni and Ag-Ni couples were increased, above those expected from expression (2), by a further variable. This extra factor is not, however, immediately obvious. Thus, although a contaminant film would give an additive term to Equation (2), it would also be expected to be present for the Ag-Ag system. Unfortunately, it is not possible to compare these results with those of other workers as no other contact resistance work has been done with surfaces of such cleanliness. Further work is obviously needed, therefore, to understand this anomaly.

Thus, the elastic area approximation seems to give a reasonable measure of the area of contact at maximum load. This view is substantiated by the theoretical analysis outlined above for the couple most inclined to plastic behavior; by the agreement with areas obtained by the contact resistance method for the Ag-Ag couple; and by the more reasonable strengths obtained for the dissimilar metal couples using the elastic method compared to the contact resistance method. It should be appreciated, however, that the above calculations assume perfectly flat or spherical specimen surfaces. In actuality there are asperities on the surfaces, which will deform plastically. The load is nevertheless carried in the bulk material by predominately elastic deformation, and this is especially so for the present case, where the specimen couples are repeatedly loaded and unloaded in the same



contact region. Thus, the asperities are deformed and the elastic deformation is increased at the expense of the plastic, due to work hardening.

## 2. Effect of Surface Cleanliness and Atmosphere on Adhesion

Figure 8 shows the effect of varying the specimen surface conditions and ambient atmosphere on the adhesion of the Ag-Ag couple under loading cycles of maximum load 1.3 - 1.6 grams. The cycles were done consecutively on the same specimens during one adhesion experiment comprising of a total of 250 cycles at different loads. Each point represents one cycle. The criteria of adhesion are, as stated above, significant joint strength as determined by the elastic contact area approximation, and the stability and maintenance of minimum contact resistance up to the breakaway point during the unloading cycle. As may be seen there is no adhesion evident with as-assembled specimen surfaces in air before evacuation; in vacuum ( $\sim 10^{-6}$  Torr) before the bakeout cycle; and in vacuum ( $\sim 5 \times 10^{-10}$  Torr) after bakeout. A preliminary electron bombardment degassing treatment of the surfaces, however, resulted in the evidence of the two contact resistance adhesion criteria, but virtually no appreciable joint strength. Significant adhesion is, however, apparent, after argon bombardment, when cycles were done in a few microns of argon; immediately after electron bombardment in high vacuum; and even after 114 hours at a pressure of about  $10^{-4}$  Torr of atmosphere. Even on subsequently admitting 40 Torr dry air, the two contact resistance adhesion criteria are still apparent after 19 hours, although the joint strengths are reduced to virtual insignificance. Re-application of vacuum conditions to the specimens, however, increases the measureable adhesion. In contrast, admittance of 40 Torr undried air results in no observable adhesion

after one hour, but, on pumping off this atmosphere, adhesion is again evident.

A similar pattern was also found for the same couple under a load range of 0.3 - 0.5 grams, and has further been obtained for the Ag-Ni couple. The retention of adhesion after admittance of 40 Torr dry air after bombardment, being, if anything, more pronounced in the latter experiment. These results are in agreement with the normally observed increase in friction as the friction specimen surfaces are cleaned and subjected to vacuum conditions (6),(19),(20), and are also compatible with the observed effects of the subsequent entry of oxygen, nitrogen, hydrogen and water-vapor atmospheres (19),(20). Oxygen and water-vapor caused the coefficient of friction to decrease, whereas the other atmospheres had no effect.

These present results demonstrate that, whereas no adhesion is evident before surface cleaning, even under ultra-high vacuum conditions, it is remarkably persistent afterwards, even after an exposure which should ensure the presence of appreciable adsorbed contaminant films. A pressure of 40 Torr air, however, effectively prevents adhesion, but the process is reversible and adhesion may be again procured by pumping off the atmosphere. Dry air seems to be much less of a barrier to adhesion than undried.

### 3. Discussion of Factors Affecting Adhesion

#### a) Mutual Solubility Criterion

The present results show no difference in the tendency to adhesion for the Ag-Ag, the immiscible Ag-Ni, and the mutually soluble Cu-Ni systems. The strength of the weakest member is approximated even at very light loads. These results are consequently at variance with earlier work by Keller and Spalvins

(9), who reported no adhesion between the Ag-Ni system under touch contact. The present results are well substantiated, however, and are thought to be more reliable than those of the earlier exploratory experiments.

It seems, therefore, that mutual solubility, per se, is no criterion for adhesion. In order to understand this, we must consider the energies involved in forming a compound between the two metals of the couple, and those involved in causing adhesion to occur between their surfaces. In the first case, if a compound is to be formed, there must be a reduction in energy of the system, i.e. the energy of the compound formed must be less than the sum of the energies of the two metals. In the latter case, however, adhesion will occur if the energy of the resultant interface is less than the sum of the surface energies of the two metals. Consequently, the condition for immiscibility involves a bulk material energy criterion, whereas the condition for adhesion requires a criterion involving surface and interfacial energies. These latter are, nevertheless, dependent on the bulk energies (21), but the relationship is, at present, unclear. Thus, no predictions concerning the ability of metal couples to adhere can, as yet, be made from their bulk interactions.

b) Elastic Relief Forces

The failure of bonds on unloading by elastic forces has been postulated by Bowden, Tabor et al (6),(22), largely in connection with metallic friction work, and this view has been widely held to explain the apparent lack of normal adhesion during friction experiments. The present work shows, however, that there is no evidence that elastic forces break the bonds

formed during unloading of the Ag-Ag, Ag-Ni and Cu-Ni couples which were contacted under high vacuum with clean specimen surfaces. In contrast, measurable adhesion and maintenance of minimum contact resistance was observed even for couples unloaded after the application of very light loads ( $< 0.1$  grams).

If total elastic deformation and ideally flat specimen surfaces are assumed, we may obtain some idea of the forces involved during elastic unloading conditions. Figure 9 shows such idealized conditions for two specimen spheres under loaded and unloaded conditions. In this case it can be shown geometrically that,

$$b = R - (R^2 - a^2)^{1/2} \quad (9)$$

where  $b$  is the vertical displacement,  $R$  the radius of the spheres, and  $a$  the radius of the contact circle.

If we now also consider the presently used Ag-Ag crossed wire specimens under a load of 1 gram, we know from Equation (3) that  $a = 3.6 \times 10^{-4}$  cms. It can be further shown, by substitution in Equation (9) and by binomially expanding, that, for this case,  $b = 1.27 \times 10^{-6}$  cms. Thus, the average separation of the two wires on unloading  $= 1.27 \times 10^{-6}$  cms, and as total metallic contact over the contact region is assumed during maximum load, it can be shown that, for maintenance of this contact area on unloading,

$$\frac{(\text{Average required extension of contact zone on unloading}(b))}{(\text{Diameter of contact zone})} = 0.2\% \quad (10)$$

This must be considered well within the ductility of most metals since Rowe (22) quotes a figure of 1-2% for model copper and brass work hardened junctions, and, consequently, it is hardly surprising

that no elastic breakaway was observed in the present clean metals couples tested in ultra-high vacuum.

The above treatment, however, neglects the fact that the real contact area consists of a number of welded asperities, which would thus give a larger value to the above ratio (10), at the outer edges of specimen contact. This would be especially so if a contaminant oxide film were present at the interface, since rupture of this film would be required before metal-metal bonding occurred. The resultant bonds would consequently be smaller and fewer in number than for clean surfaces. Thus, rupture of bonds by elastic relief forces would be more evident in contaminated surfaces than clean surfaces. This could explain why no measurable joint strengths were observed in the Ag-Ag couple after initial electron degassing bombardment, under high vacuum, Figure 8, although the two contact resistance adhesion criteria were observed up to the breakaway point. It is thought that the oxide and other contaminant films were not sufficiently removed by this treatment, thus allowing elastic relief forces to break the bond under zero loading conditions, but sufficient being removed to give some indication of adhesion. Such an explanation could also be given to Bowden and Rowe's results (6) on the welding of Au-Au, Ni-Ni, Pt-Pt and Ag-Ag couples in a vacuum of  $\sim 10^{-8}$  Torr, after surface cleaning by extensive evaporation. They observed no appreciable adhesion when these couples were subjected to normal loads of less than 15 grams, and it is possible that all contaminants were not removed (3).

Thus, although none of the bonds between clean metal

couples, in the presented experiments, appeared to be broken by the relief of elastic forces, even after the application of very light normal loads, it is felt that the effect of these forces may be more pronounced for contaminated surfaces, and also, of course, for harder metals.

c) Effect of Contaminants

The present experiments show that there are two classes of contaminants which prevent adhesion, those contaminants present in the surrounding atmosphere, which can be pumped off with the consequent reappearance of adhesion, and those which cannot be pumped off. The first class consists of gases and volatile compounds, in the present case: oxygen, carbon dioxide, nitrogen and water vapor, and the second of stable surface films such as oxides.

If we consider the presented Ag-Ag results shown in Figure 8, the effect of the stable films becomes evident. Thus, no adhesion was observable under a vacuum of  $\sim 5 \times 10^{-10}$  Torr, even after a bakeout cycle of 10 hours at 450°C, which would have removed all but the most tightly held adsorbed films. Consequently, oxide-oxide bonding must be discounted in these, and subsequent, cycles, since if it were to occur, it should do so here after such a rigorous treatment. Metal-metal contact, however, was thought to occur during these tests under loaded conditions, since the contact resistance measurements gave values only about twice as great as those for the cleaned surfaces in high vacuum. The barrier to adhesion in this case, therefore, seems to be that mentioned in the previous section, namely, fracture of the metal-metal bonds, formed through the fragmented oxide layers,

by elastic relief forces as the load is removed. It seems unlikely that sufficient mobile contaminants would be present at the interface to prevent the adhesion of the virgin metal contacts, in the manner described by Nicholas and Milner (23) for metals welded in the atmosphere, after such a rigorous bakeout cycle.

The effect of gaseous contaminants, however, is different. Since the barrier to adhesion here is reversible, it seems that these must prevent the adhesion of the virgin metal contacts extruded through the stable contaminant films. Thus, an adsorbed water film on the surface would constitute a highly mobile film, difficult to disperse to form metal-metal contact. Indeed water vapor seems to be the most effective barrier to adhesion of all the atmospheres studied. Thus, an ambient pressure of 40 Torr of dry air has less effect in preventing adhesion than 40 Torr of normally wet air, Figure 8. The inert argon atmosphere, however, has no discernable effect, and it must also be assumed that the nitrogen and carbon dioxide present in the air atmosphere behave likewise. Oxygen, however, being a more reactive gas might be expected to be more effective in "poisoning" the extruded metal contacts. The adhesion, however, seems to be remarkably persistent after the surfaces have been cleaned, being significant after a 14 hour exposure to a pressure of  $\sim 10^{-4}$  Torr air, Figure 8. It seems, therefore, that even under the light loads of the present experiments, adhesion was not prevented by significant amounts of adsorbed and stable contaminant films.

The present work, therefore, substantiates the view that the dispersal of contaminants is the prime barrier to adhesion

of solid metal couples. Since adhesion was observed for cleaned surfaces under high vacuum with the application of extremely light loads, it must be assumed that the energy barrier to adhesion, proposed by Erdmann-Jesnitzer et al (24) and Semenov (5), due to the work needed to realign the metal surface atoms to form an interfacial bond, must be of minor importance.



## CONCLUSIONS

The role of contaminants during metallic adhesion has been clarified as a result of this work. Thus, if metal couples are placed together under virtually contaminant free conditions, they should weld spontaneously to give a strength determined by the contact area and the bulk strengths of the constituents, even in cases where the deformation is predominantly elastic. The relief of elastic forces on unloading, and the energy barrier needed to reorientate the surface atoms to form an interface are of minor importance under such conditions, at least for the softer materials studied here.

The presence of contaminants at the interface may limit adhesion in two ways. If the contaminant is in the form of a stable surface layer, of above minimum thickness, such as an oxide film, it is thought that, although bonds may be formed between the virgin metal contacts extruded through the fractured oxide layer under lightly loaded conditions, they break on unloading the couple. They do this because of the relief of elastic forces, which becomes important in this case because of the restricted size of the metal-metal contact points. If the more mobile adsorbed gaseous or liquid films are present, however, bonding between such metal contact extrusions is thought to be eliminated at light loads, even under loaded conditions. The effect on adhesion of these mobile contaminants is, however, reversible for initially clean surfaces, i.e. adhesion can often be reasserted by removing the atmosphere surrounding the adhesion couple, whereas a rigorous cleaning procedure is required to remove the more stable surface films. Heavy bulk deformation, however, would enable the dispersal of such films, ensuring consequent bonding, as is commonly encountered on the pressure welding of metals in air.

The miscibility criterion of adhesion of dissimilar metal couples does

not apply to the insoluble Ag-Ni couple studied, and is thought to be of only secondary importance, since it is only a bulk criterion. Adhesion, however, concerns surface and interfacial energies, and these are of unknown magnitudes.

# REFERENCES

- (1) F.P. Bowden, and D. Tabor, The Friction and Lubrication of Solids, Clarendon Press, Oxford, England (1950).
- (2) G. Salomon, and R. Houwink, Adhesion and Adhesives, Vol. 1, Elsevier Pub. Co., Amsterdam, Holland (1965).
- (3) D.R. Milner, and G.W. Rowe, Met. Rev., 7, No. 28, 433 (1962).
- (4) M.E. Sikorski, Mechanisms of Solid Friction, Eds. P.J. Bryant, M. Lavik and G. Solomon, Elsevier Pub. Co., Amsterdam, Holland (1964).
- (5) A.P. Semenov, Wear, 4, 1 (1961).
- (6) F.P. Bowden, and G.W. Rowe, Proc. Roy. Soc., 233A, 429 (1955).
- (7) J.L. Ham, Trans. Amer. Soc. Lub. Eng., 6, 20 (1963).
- (8) C.E. Moeller, J. Bossert, and M. Noland, Cold Molecular Welding Study in Ultra-High Vacuum, Final Report Midwest Research Institute, Missouri, Project No. 2817-E (1965).
- (9) D.V. Keller, Jr., and T. Spalvins, Trans. Vac. Met. Conf., Ed. R.F. Bunshah (1962), Amer. Vac. Soc. Pub. 149, Boston (1963).
- (10) A.W. DeGee, Wear, 8, 121 (1965).
- (11) A.E. Roach, C.L. Goodzeit, and R.P. Hunnicut, Trans. Amer. Soc. Mech. Eng., 78, 1659 (1956).
- (12) K.J.B. McEwan, and D.R. Milner, Brit. Weld. J., 9, 406 (1962).
- (13) J.B.P. Williamson, Proc. Inst. Elec. Eng., 109A, No. 3, 224 (1962).
- (14) M. Hansen, Constitution of Binary Alloys, McGraw-Hill Book Co., Inc., N.Y. (1958).
- (15) R. Holm, Electric Contacts Handbook, Springer-Verlag, Berlin, Germany (1958).
- (16) H. Hertz, see S. Timoshenko and J.N. Goodier, Theory of Elasticity, McGraw-Hill Book Co., Inc., N.Y. (1951).
- (17) D. Tabor, The Hardness of Metals, Clarendon Press, Oxford, England (1951).
- (18) Metals Handbook, Amer. Soc. Metals (1948).
- (19) F.P. Bowden, and T.P. Hughes, Proc. Roy. Soc., 172A, 263 (1939).
- (20) F.P. Bowden, and J.E. Young, Proc. Roy. Soc., 208A, 311 (1951).
- (21) D.V. Keller, Jr., Internat. Auto. Eng. Cong., No. 985A (1965).

REFERENCES (Cont'd.)

- (22) F.P. Bowden, and D. Tabor, The Friction and Lubrication of Solids, Park II, Clarendon Press, Oxford, England (1964).
- (23) M.G. Nicholas, and D.R. Milner, Brit. Weld. J., 9, 469 (1962).
- (24) F. Erdmann-Jesnitzer, Aluminum, 33, 730 (1957).

#### ACKNOWLEDGEMENTS

The authors wish to acknowledge the financial support of this program by the National Aeronautics and Space Administration, and the Sandia Corporation.

## FIGURE CAPTIONS

- Figure 1 - Diagrammatic sketch of vacuum system where, A is the adhesion cell, B the electrical leads into the cell, C the strain gauge leads, D the Redhead gauge, E the titanium sorption pump, F the argon source, G the conflat flanges, H the 1" Granville-Phillips valve, I the 300 mm liquid nitrogen traps, J the Pyrex-Kovar seals, and K the 1/2" Granville-Phillips valve.
- Figure 2 - Diagrammatic sketch of adhesion cell where, A is the sample plate, B the sample indenter, C the positioning magnet, D the Redhead gauge, E a filament, F the iron slugs, G the strain gauge assembly, H the argon capsule, I the titanium sorption pump, J the calibrated variable resistance, K the 1/2" Granville-Phillips valve, and L the load solenoid.
- Figure 3 - Adhesion cycles of the Ag-Ag system:  
 (a)  $5 \times 10^{-10}$  Torr, after bakeout, before surface bombardment.  
 (b)  $\sim 10^{-4}$  Torr of argon, 24 hrs. after argon ion bombardment.
- Figure 4 - Contact resistance at maximum load vs the maximum load on the couple, for adhesion cycles at  $\sim 5 \times 10^{-10}$  Torr, after argon ion and electron bombardment.
- Figure 5 - Joint strength - indentation load relationship for the Ag-Ag couple, the joint strength being calculated from the contact resistance approximation of the area of contact. Pressure  $\sim 5 \times 10^{-10}$  Torr, after argon ion and electron bombardment.
- Figure 6 - Average pressure,  $P_m$ , vs load for an idealized indentation.
- Figure 7 - Joint strength - indentation load relationship for the Ag-Ag couple, the joint strength being calculated from the elastic approximation of the area of contact. Pressure  $\sim 5 \times 10^{-10}$  Torr, after argon ion and electron bombardment.
- Figure 8 - Joint strengths of the Ag-Ag couple under various atmospheric and surface conditions, the joint strengths being calculated from the elastic approximations of the areas of contact. The lines A and B represent the stability of the contact resistance to contact break, and the maintenance of the minimum resistance, respectively, during the unloading cycle. Load on the couples; 1.3 - 1.6 grams.
- Figure 9 - Idealized cross-section of specimen spheres under loaded (dotted lines) and unloaded (full lines) conditions.

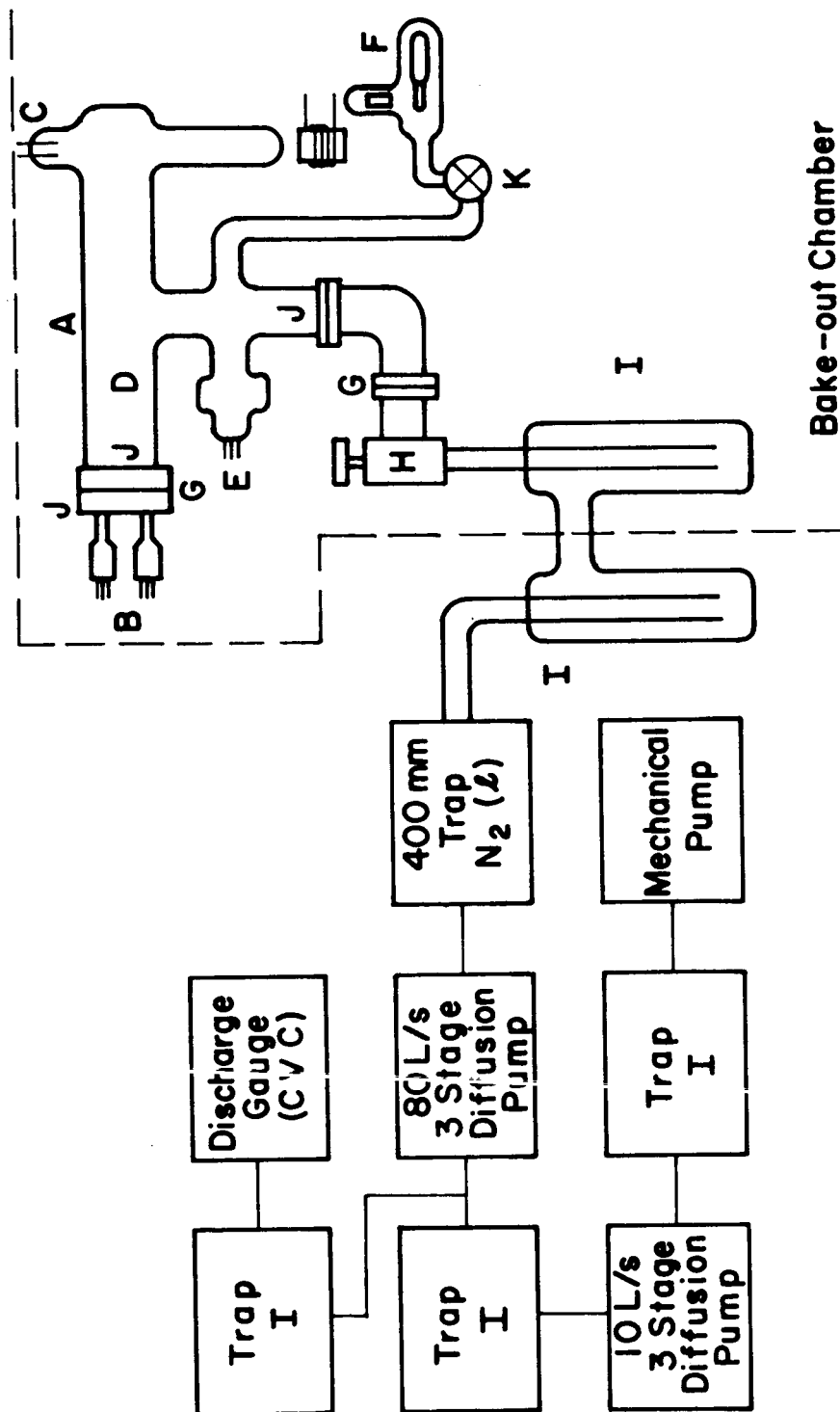


FIGURE 1

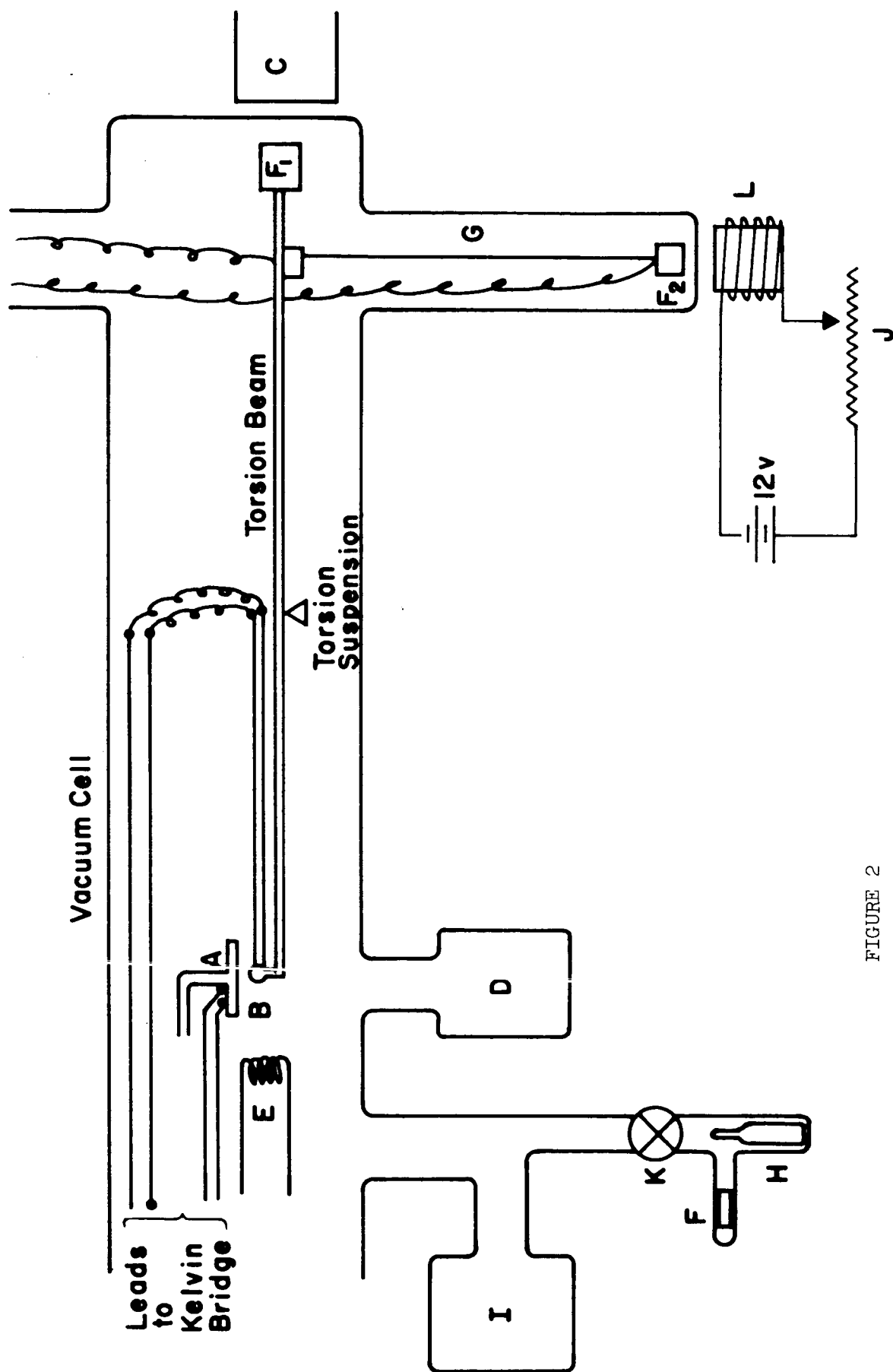


FIGURE 2



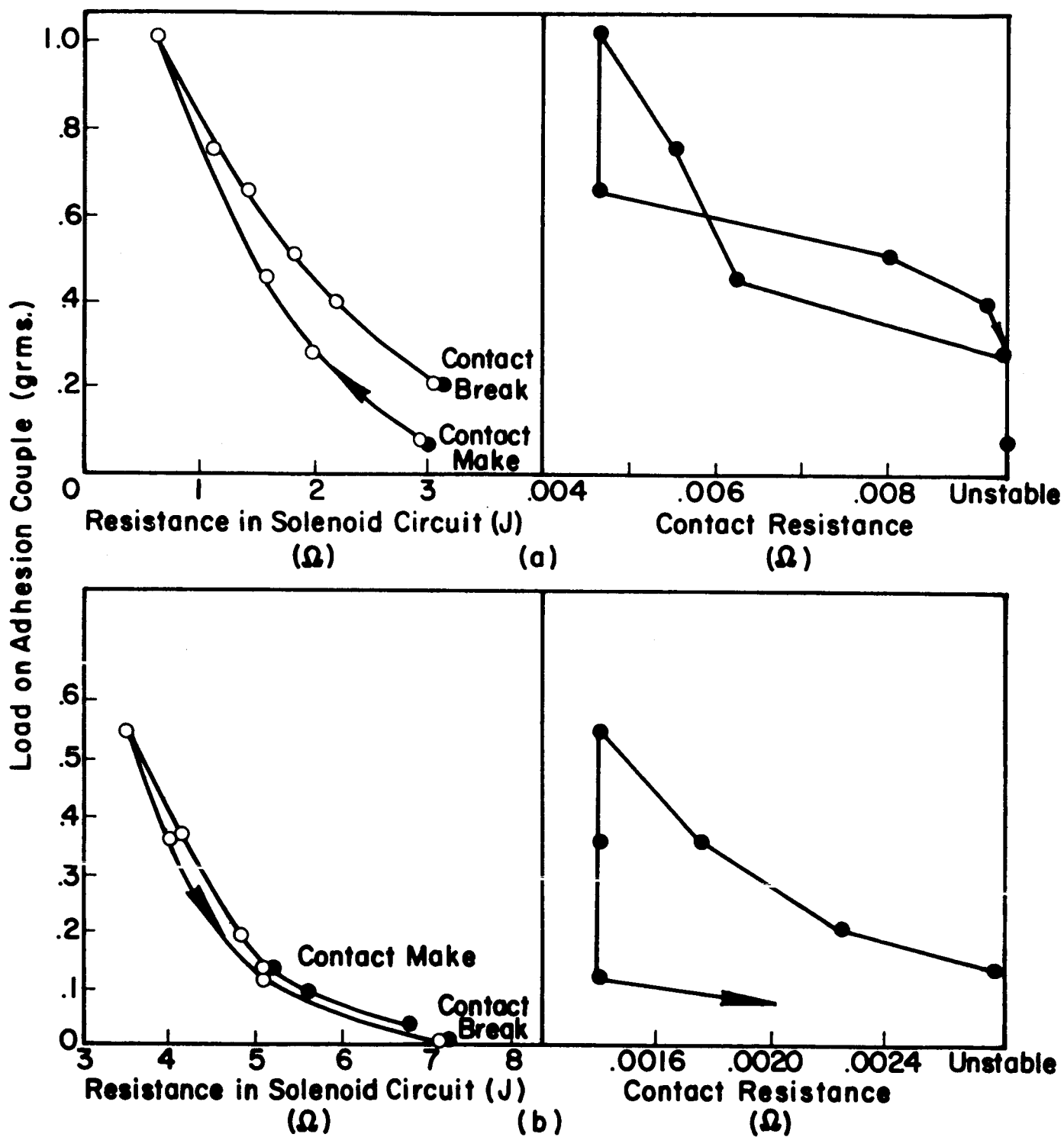


FIGURE 3

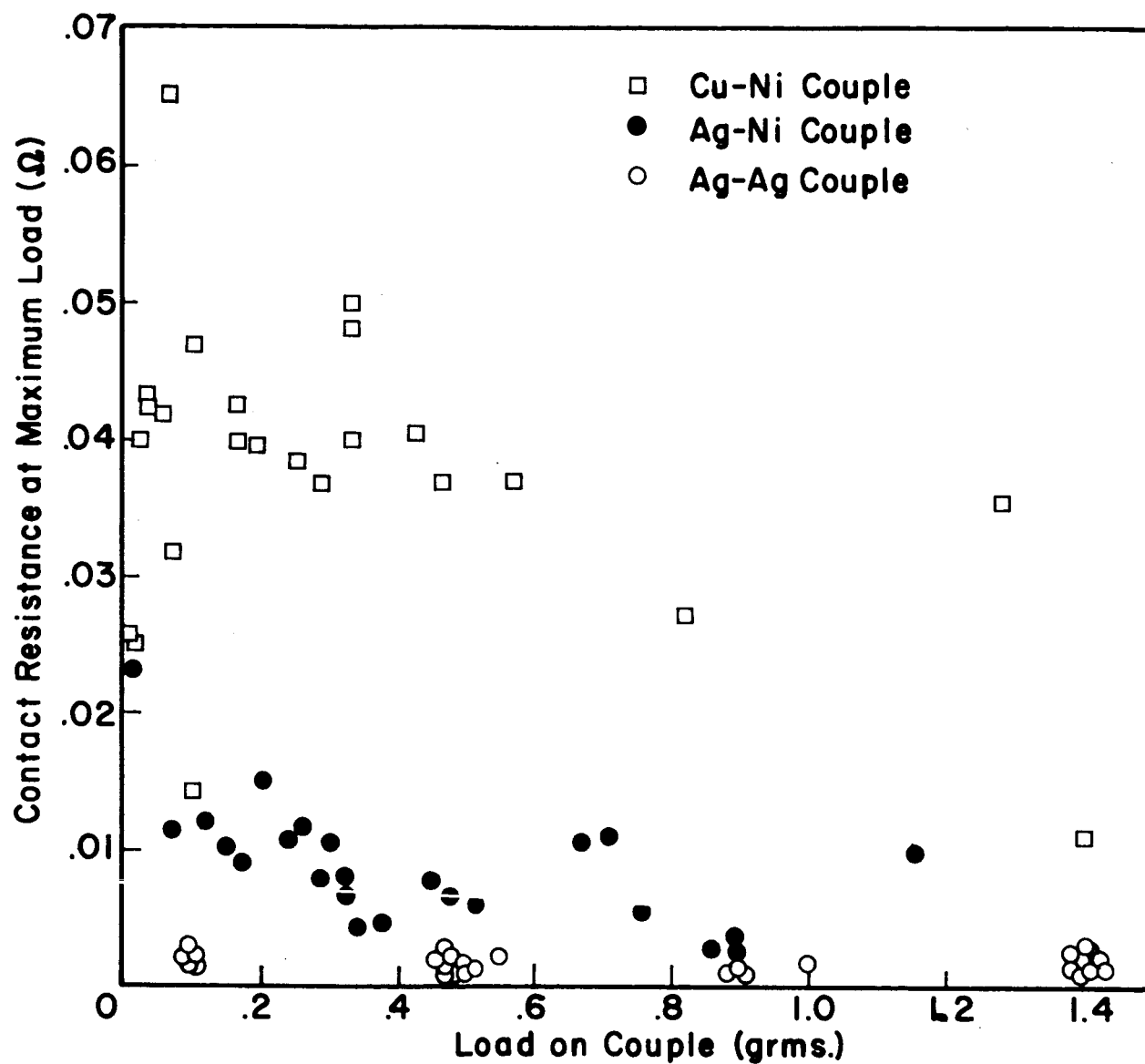


FIGURE 4

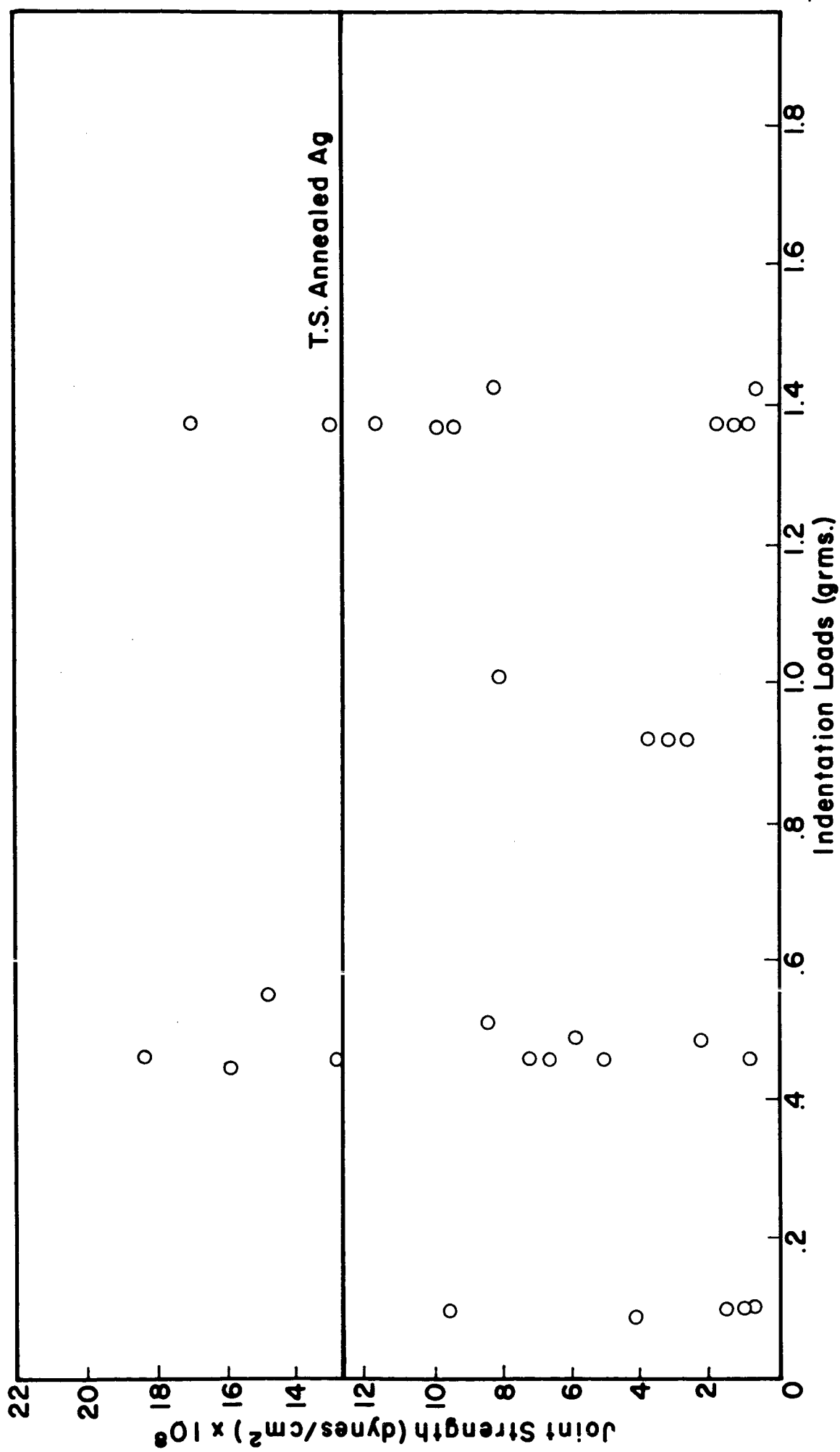


FIGURE 5

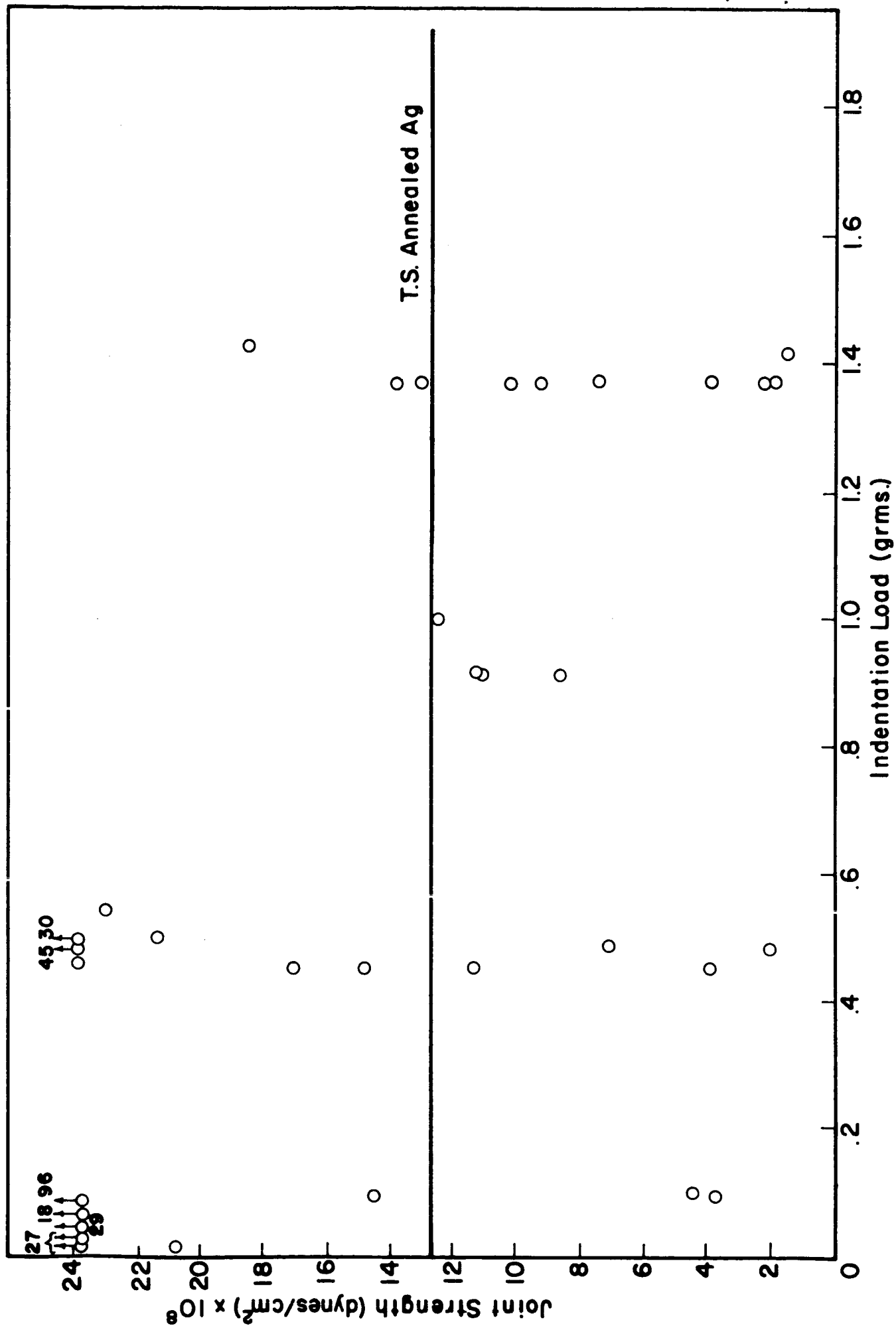


FIGURE 7

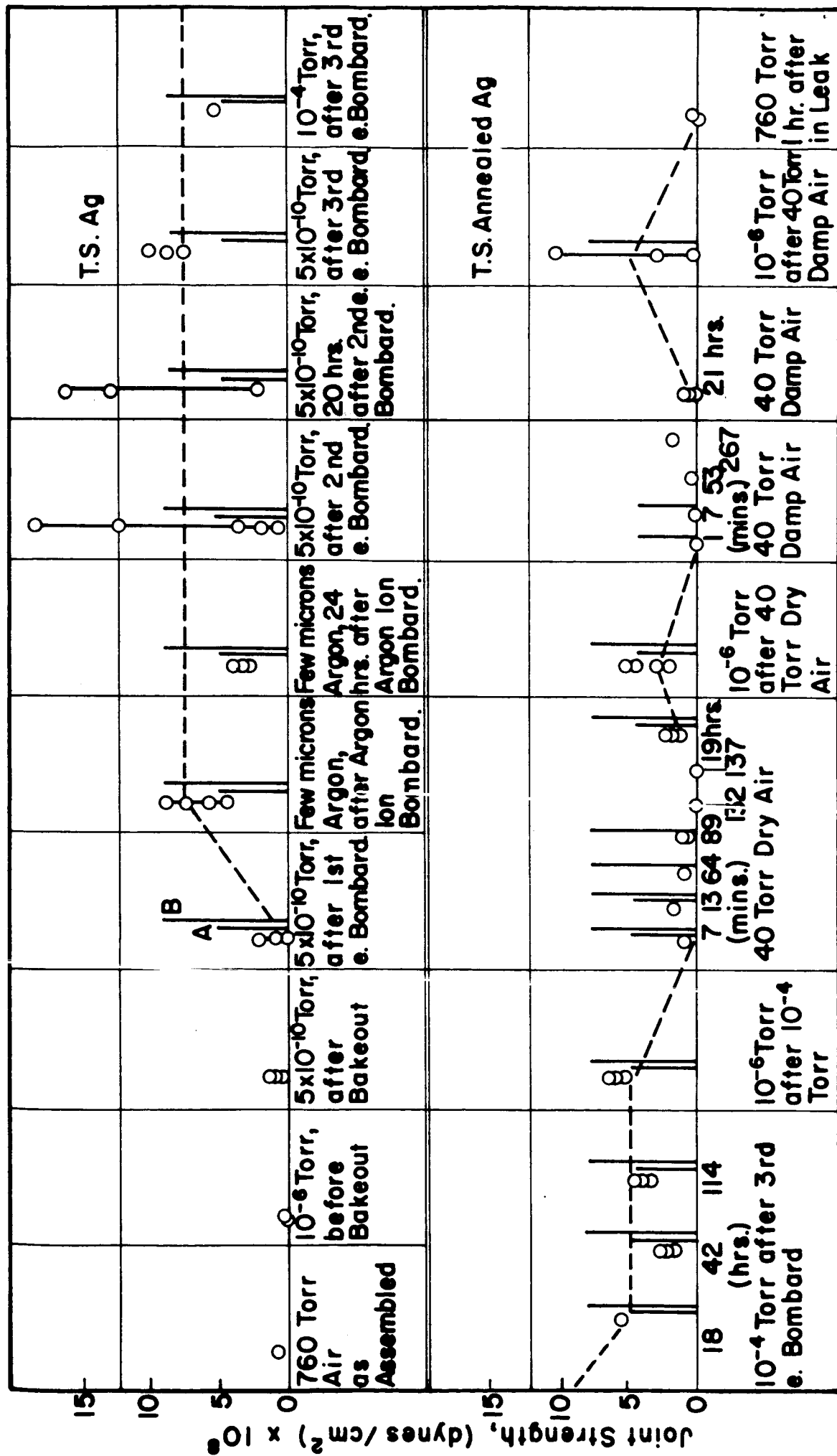


FIGURE 8

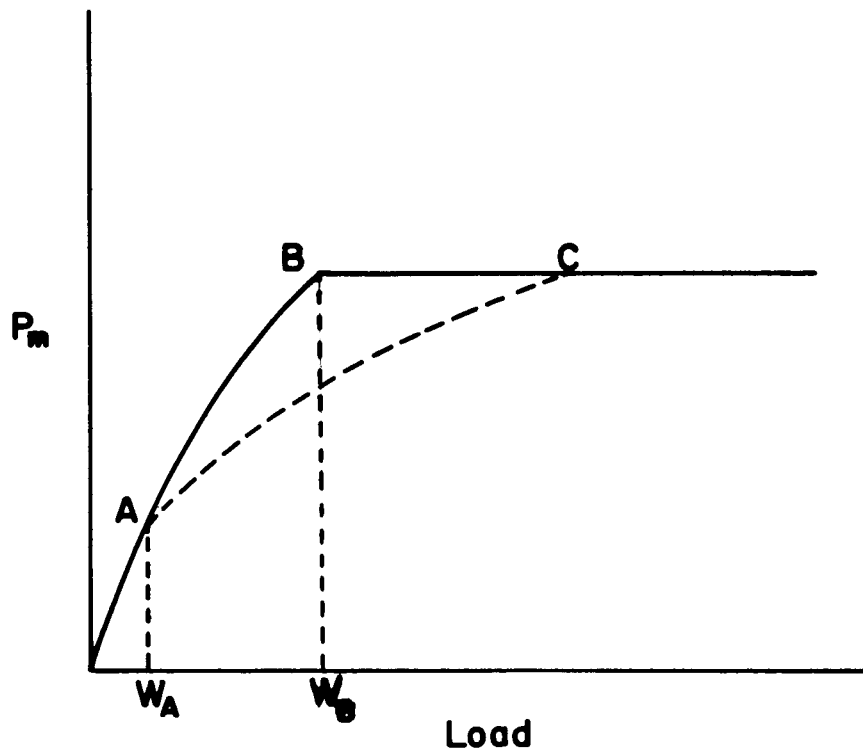


FIGURE 6

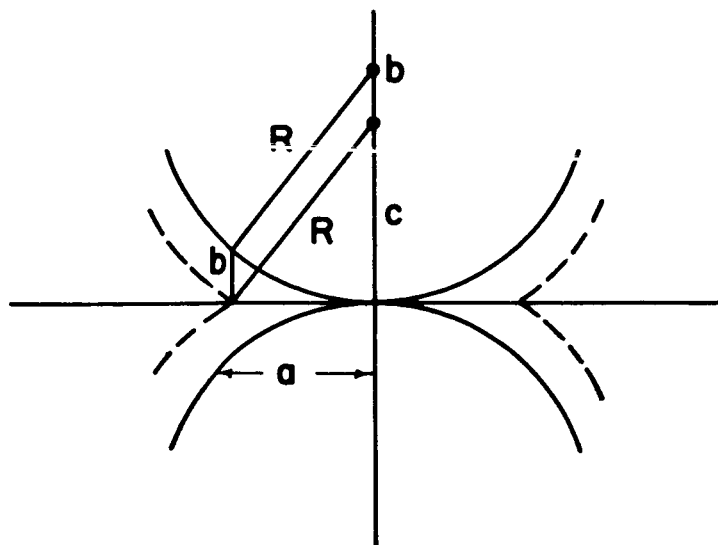


FIGURE 9